ORIGINAL ARTICLE

Biomarker characteristics of the Turonian–Eocene succession, Belayim oilfields, central Gulf of Suez, Egypt

CrossMark

W.Sh. El Diasty [a], A.A. Abo Ghonaim [a], A.R. Mostafa [b], S.Y. El Beialy [a,*], K.J. Edwards [c]

[a] Geology Department, Faculty of Science, Mansoura University, Mansoura, Egypt
[b] Environmental Sciences Department, Alexandria University, Alexandria, Egypt
[c] School of Geosciences, University of Aberdeen, Aberdeen, UK

Abstract   This study assesses the hydrocarbon source rocks of the Belayim oilfields, central Gulf of Suez, Egypt. Detailed geochemical methods, including liquid chromatography, gas chromatography and gas chromatography–mass spectrometry, are used to characterize organic-rich facies of the Turonian–Eocene deposits. Crude oil samples are analyzed using C_7 and stable carbon isotopes, in addition to analysis of the extracts, in order to throw light on the organic matter source, composition, and thermal maturity. The source rocks are mainly derived from algae and bacteria deposited under normal saline and reducing palaeoenvironmental conditions, with a minimal contribution from terrestrial organic and mainly clay-poor source rocks. This is evidenced by the n-alkane distribution, the pristane/phytane, homohopane, gammacerane index, the high concentration of cholestane, the presence of the C_{30} n-propylcholestanes and low diasteranes ratios. The source rock extracts range from immature to marginally mature, based on biomarker maturity-related parameters. A similar scenario is envisaged from the crude oil samples which showed a partial positive correlation with the source rocks of the Eocene Thebes Formation, and the Upper Cretaceous Brown Limestone. Our data suggest that Turonian–Santonian Matulla Formation samples may signify the presence of some oil in the study area.

© 2014 Production and hosting by Elsevier B.V. on behalf of University of Bahrain.

1. Introduction

The first oil discovery on the Gemsa Peninsula, Gulf of Suez, Egypt was in 1886. This was followed by intensive exploration which eventually resulted in the discovery of more than 120 oilfields providing more than 50% of the overall daily oil production of the country (Egypt Country Analysis Briefs, 2009). The Belayim development leases (about 260 square km) in which the two oilfields of Belayim Marine and Belayim Land are located, represent one of the largest oil accumulations in the Gulf of Suez (Fig. 1).

* Corresponding author. Tel.: +20 109 3840625.
  E-mail address: syelbeialy@mans.edu.eg (S.Y. El Beialy).

Geological and geochemical evidence has shown that carbonate rocks are the source of the Gulf of Suez oils. Identification of possible source rock facies in the crude oils using routine geological criteria and bulk geological data, proved inconclusive in this supposition. More recently, the use of biological fossils (or biomarkers) in conjunction with bulk parameters was effective in the evaluation of the source rocks and the genetic classification of oils in the Gulf of Suez.

Biomarkers such as hopanes and steranes have received much attention because of their usefulness as indicators of organic matter type and quality, depositional conditions (e.g. salinity, oxicity, anoxicity, etc.), assessment of maturity level, extent of biodegradation and lithology. Such features make biomarkers potentially applicable to oil–oil correlations. With the increased need to improve the success of petroleum exploration and to reduce risk, the characterization of oils using biomarkers and isotope geochemistry has provided a new impetus to the evaluation of petroleum systems, plays, and prospects. Molecular geochemistry can assist in ascertaining the depositional environment of petroleum source rocks via the types of contributing organisms in their related oils (e.g. Moldowan et al., 1985; Mello et al., 1988; Peters et al., 2005; Roushdy et al., 2010; El Diasty and Peters, 2014). The central Gulf of Suez and adjacent areas have been subjected to extensive geochemical studies in order to evaluate the oils and their related source rocks (Rohrback, 1983; Mostafa, 1993; Barakat et al., 1997; El Diasty and Peters, 2014). Very few, if any, of these studies have dealt with the study of source rock generating potential and its correlation with the oil being recovered from reservoirs. The richness assessment of the

source rock is not estimated in the current study as this will be discussed in a forthcoming paper. Our analyses showed that the source rocks encountered are rich enough to generate hydrocarbons at optimum maturity. This paper focuses on the use of detailed biomarker data in a trial to: (1) evaluate the hydrocarbon potential and thermal maturity of the Upper Cretaceous-Eocene subsurface deposits in the Belayim oilfields; (2) envisage organic matter source, depositional environment and redox conditions; and (3) elucidate the geochemical characteristics of the local oil, in addition to correlating them with the source rock parameters.

2. Geological setting

The Gulf of Suez represents one of the most intensively faulted areas on Earth. It is approximately 300 km long with an average width of 70 km and it forms the northern extension of the Red Sea, covering an area of about 25,000 square km at an average water depth of 55–100 m (Young et al., 2000). It extends NW of 27°30′ N to 30°00′ N, and its width varies from about 50 km at its northern end to about 90 km in the south where it merges with the Red Sea (Bosworth and McClay, 2001). Tectonic subsidence and sedimentation were slow during the initial phase of rifting which was related to the separation of the African and Arabian plates (Meshref, 1990) during the latest Oligocene to the Early Miocene (ca 24–15.5 Ma). The Gulf of Suez is the main oil-producing province in Egypt, with oil being produced from Paleozoic, Mesozoic and Cenozoic rocks. The lithostratigraphic units in the Gulf of Suez range in age from Precambrian to Holocene. The succession can be divided into three lithostratigraphic megasequences (Plaziat et al., 1998). The units include: (i) a pre-rift (pre-Miocene or Paleozoic–Eocene, e.g. Schütz, 1994) succession including basement; (ii) a syn-rift (Oligocene–Miocene) interval (Al-Husseini, 2012); and (iii) a post-rift (post-Miocene or Pliocene–Holocene) interval (Alsharhan, 2003). These units vary in thickness, lithology, areal distribution, depositional environment, and hydrocarbon importance (Alsharhan, 2003). The lithostratigraphic successions of the Belayim Land and Belayim Marine are shown in Fig. 2 as reported by Petrobel (2005).

This paper concentrates on the middle and upper parts of the pre-rift interval, which comprises the Nubian Complex (Paleozoic-Lower Cretaceous) at the base, overlain by a Cenomanian–Late Eocene sequence (Alsharhan, 2003). The Nubian (or Nubia) Sandstone describes the Paleozoic–Cretaceous clastic succession which overlies unconformably the basement complex, as in the Belayim Marine oilfield. This is followed by an Upper Cretaceous succession consisting of four formations (Raha, Abu Qada, Wata, and Matulla) arranged from base to top (Fig. 2). This sequence is in general composed of coarse sandstones and shallow-marine dolomitic limestones with interbedded shales. From the Cenomanian through the Turonian, deposition took place largely in a restricted, shallow-marine, inner sub-littoral environment (Schütz, 1994). This is overlain by the Brown Limestone/Sudr Chalk (Campanian–Maastrichtian) deposited in marine sub-littoral contexts with less organic-rich sediments (Schütz, 1994).

The top of the pre-rift succession is terminated by the Eocene Thebes Formation, an argillaceous limestone unit with
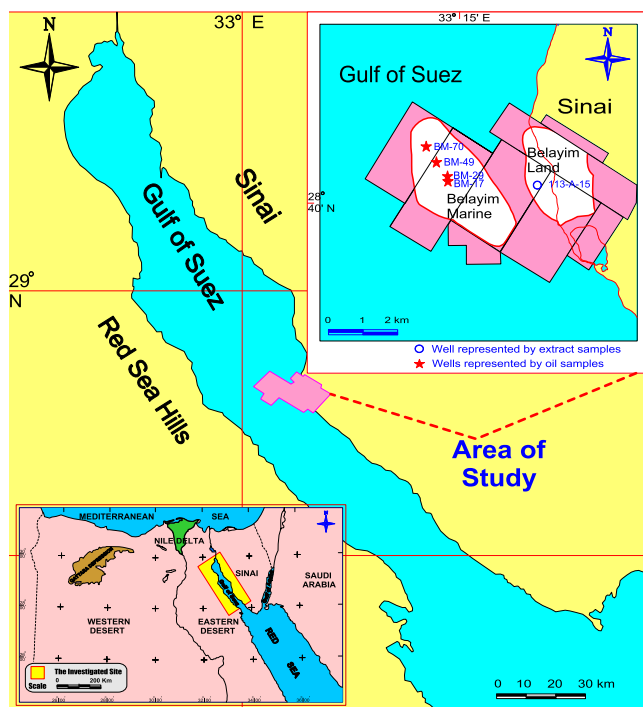

Figure 1   Location map of the studied wells, Belayim oilfields, central Gulf of Suez, Egypt.
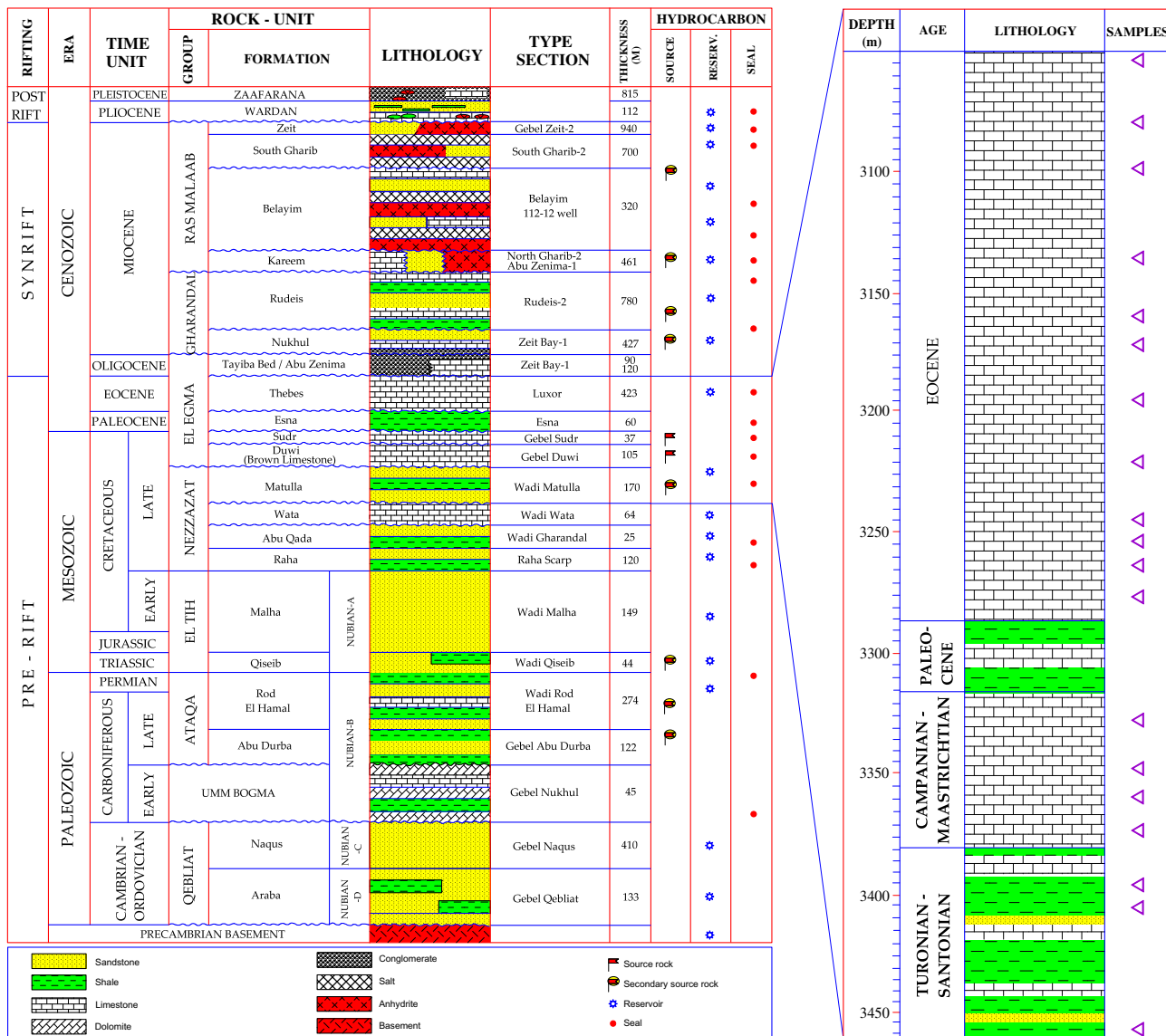
Figure 2 Correlation of the BL 113-A-15 well, Belayim Land oilfield (Petrobel, 2005) with the generalized lithostratigraphic column of Alsharhan (2003).

subordinate shales and sandstones, and was deposited in a marine outer sub-littoral setting (Schütz, 1994). It rests conformably on the Paleocene Esna Shale. Oil is produced from the Eocene carbonates in the Bakr and Sudr fields. There is no possibility of the shale (Fig. 2) being a source for the oil in the study area. In the southern Gulf of Suez, the Miocene Rudeis and Kareem formations act as active source rocks (Bakr and Wilkes, 2002; El Diasty and Peters, 2014).

3. Materials and methods

Nineteen ditch cuttings collected from the BL 113-A-15 Well, in addition to 4 oil samples retrieved from the BM-17, BM-29, BM-49 and BM-70 wells in the Belayim Marine and Belayim Land oilfields (Fig. 1), were considered for organic geochemical analyses involving the following methods:

1. Extraction of bitumens: these were extracted by dichloromethane (CH_2Cl_2) according to the methods of Ganz et al. (1990).
2. Liquid chromatography: this involved the fractionation of extracts and oils by column chromatography, where asphaltenes were precipitated with hexane and the soluble fraction was separated into saturates, aromatics, and resins (NSO compounds) on a silica–alumina column by successive elusion using hexane, benzene, and benzene–methanol. The solvents were evaporated and the weight percentage of each component was determined.
3. Gas chromatography (GC): this was carried out on the extract and oil samples, using a Hewlett Packard 5890 gas chromatograph fitted with a Quadrex 30-m fused silica capillary column (0.25 mm internal diameter, 0.25 μm film thickness). The GC is programed from 40 to 340 °C at 10 °C/min with a 2 min hold at 40 °C and a 20 min hold at 340 °C.
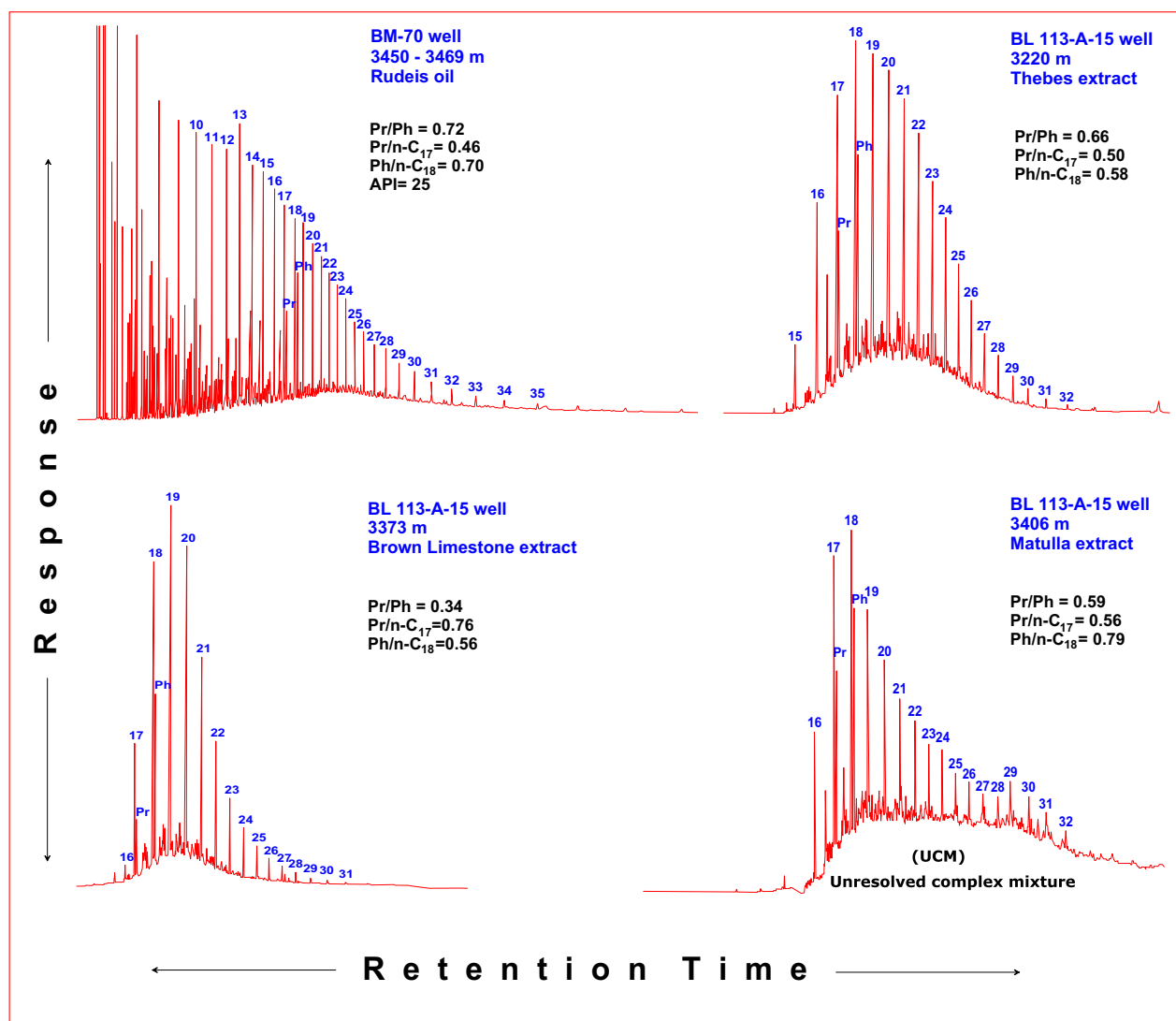
Figure 3 Gas chromatograms of the Eocene and Upper Cretaceous extract and oil samples in the Belayim oilfields.

4. Gas chromatography–mass spectrometry (GC–MS): saturated fractions of extracts and oils were injected into a HP5890 gas chromatograph coupled to a HP5971A Mass Selective Detector (MSD). The capillary column dimensions were 30 m × 0.25 mm internal diameter and helium was used as a carrier gas. The temperature was programed from 50 to 140 °C at 40 °C/min and further to 320 °C at 2 °C/min with a final hold time of 30 min. The analysis of the saturated fractions involved two important hydrocarbon classes: terpanes with mass/charge m/z (191) and steranes with m/z (217). The relative contents of particular compounds were calculated from peak areas.

5. High resolution C_7 light hydrocarbon analysis: this required a direct injection into a Varian 3400 gas chromatograph fitted with a split injector and Quadrex (100 m × 250 μm I.D. × 0.5 μm film thickness) fused silica capillary column. The GC run was isothermal at 35 °C, while collecting data from C_2 to C_7. Analytical data were processed with a Nelson Analytical model 3000 chromatographic data system and IBM computer hardware.

4. Results and discussion

4.1. Molecular composition of bitumen

The gas chromatography (GC) analysis (Fig. 3) was used to interpret environmental conditions at the time of deposition and the source of the organic matter (Tissot and Welte, 1984; Moldowan et al., 1985) was based on the distribution of n-alkanes and isoprenoids. The GC results for 5 samples from different formations encountered in the 113-A-15 Well are summarized in Table 1, along with gas chromatograms showing a front end biased distribution of the n-alkanes in the extract samples (Fig. 3). This is typical of oils derived from source rocks with a contribution from marine algae (kerogen type II), deposited under anoxic marine conditions with no obvious contribution from terrestrial higher plants.

GC can provide general information to map the regional, vertical and temporal extent of contamination to assess the effectiveness of biodegradation (Peters et al., 2005). Peculiarly,

Table 1 Results of liquid chromatography and gas chromatography of samples from the BL 113-A-15 well, Belayim Land oilfield.

No.	Depth (m)	Formation	%Sat.	%Aro.	%NSO + ASPH.	Pr/Ph	Pr/n-C$_{17}$	Ph/n-C$_{18}$
1	3051	Thebes	68.90	20.69	10.34	ND	ND	ND
2	3083	Thebes	58.90	21.79	19.23	ND	ND	ND
3	3100	Thebes	59.40	17.19	23.44	ND	ND	ND
4	3136	Thebes	54.63	16.49	28.86	ND	ND	ND
5	3160	Thebes	54.78	12.90	27.83	ND	ND	ND
6	3172	Thebes	54.28	20.00	25.71	ND	ND	ND
7	3196	Thebes	55.36	19.64	25.00	ND	ND	ND
8	3220	Thebes	23.17	09.76	67.07	0.66	0.50	0.58
9	3244	Thebes	41.90	18.09	40.00	ND	ND	ND
10	3256	Thebes	48.33	18.33	33.33	ND	ND	ND
11	3268	Thebes	56.98	21.50	21.50	ND	ND	ND
12	3274	Thebes	55.22	17.91	26.86	0.70	0.50	0.59
13	3325	Brown Limestone	61.02	18.64	20.34	ND	ND	ND
14	3349	Brown Limestone	ND	ND	ND	ND	ND	ND
15	3361	Brown Limestone	58.02	19.75	22.22	0.62	0.44	0.53
16	3373	Brown Limestone	15.38	23.08	61.54	0.34	0.76	0.56
17	3397	Matulla	59.32	18.64	22.03	ND	ND	ND
18	3406	Matulla	70.58	08.82	20.59	0.59	0.56	0.79
19	3463	Matulla	65.30	20.41	14.28	ND	ND	ND

ND: No data.

some of the BL 113-A-15 Well extracts have experienced a slight-moderate biodegradation (e.g. Matulla extract, 3406 m). It has been associated with a hump (Fig. 3) or Unresolved Complex Mixture (UCM). However, biodegradation is limited in most marine environments by sub-optimal levels of biologically available nitrogen, phosphorous and other trace nutrients (Peters et al., 2005).

The pristane/phytane (Pr/Ph) ratio is used as a biomarker parameter for assessing redox conditions during sediment accumulation. The samples are characterized by relatively high concentrations of phytane and low Pr/Ph ratios (0.34–0.70; Table 1) in the extracts from the Brown Limestone and Thebes formations. It should be noted that light hydrocarbons are missing in the extract from 3373 m especially. This could explain the very low Pr/Ph value for that sample (0.34) as pristane may have been lost by evaporation. These samples seem to have originated from a marine organic source deposited under anoxic carbonate environments (Didyk et al., 1978; Peters et al., 2005). This low Pr/Ph ratio in the Brown Limestone and Thebes Formation could also be due to rich organic sulfur (Mostafa, 1993).

An isoprenoid pristane/n-C$_{17}$ versus isoprenoid phytane/n-C$_{18}$ cross plot is used to determine kerogen type, maturation and biodegradation of the depositional environment (Peters et al., 2005; Alaug et al., 2013). Fig. 4 suggests that 4 samples from the Belayim Land oilfield are located within the zone in which marine organic matter (kerogen type II) was preserved under a reducing environment with a low maturity level. Only one sample from the Upper Cretaceous was located within the maturation zone, but in the reducing section (Fig. 4), reflecting the accumulation of mixed organic matter (kerogen type II/III).

4.1.1. Source and depositional environment-related biomarkers

Triterpanes (m/z 191) and steranes (m/z 217) are the most significant compounds capable of yielding very specific information regarding source and depositional environment as they are closely related to compounds occurring in living organisms. Biomarker ratios and indices of triterpanes and steranes

encountered in different formations of the BL 113-A-15 Well are shown in Tables 2 and 3.

The tricyclic terpanes are considered to be the diagenetic products of prokaryote membranes (Ourisson et al., 1982). Our results showed that concentrations of C$_{23}$ tricyclic terpanes in the Thebes, Brown Limestone and Matulla formations are significantly high. This may indicate that the samples are mainly of marine origin as found by Aquino Neto et al. (1983). Furthermore, the C$_{26}$/C$_{25}$ tricyclic terpane ratios have low values (0.33–0.77, Table 2) which are less than 0.9 (Peters et al., 2005), indicating a prevalent marine depositional environment. The abundant C$_{24}$ tetracyclic terpanes indicates a high contribution of bacterially-derived hopanes and a carbonate–evaporitic depositional environment with a minimal contribution from terrigenous material (Palacas et al., 1984; Mello et al., 1988).

The pentacyclic triterpanes are represented in the present work by the hopanes and the homohopanes. On the other hand, the homohopanes C$_{31}$–C$_{35}$, that occur as doublets or stereoisomeric pairs, commonly show either a regular stair-step progression, or an irregular progression in which C$_{35}$ homohopanes are more abundant than adjoining C$_{34}$ counterparts which may reflect different types of bacterial input. Samples having C$_{35}$/C$_{34}$ values > 0.8 represent marine carbonates or evaporites (Peters et al., 2005). Our well data produced values of 0.9–1.53, indicating a hypersaline, anoxic carbonate environment of deposition with no available free oxygen (ten Haven et al., 1992; Mostafa, 1993).

In contrast to hopanes, moretanes seem to be abundant in organic materials of terrestrial origin (Mann et al., 1987). The lower abundance of moretane relative to hopane may reflect a weak terrigenous input. The ratios of 17β(H),21α(H)-moretanes to corresponding 17α(H),21β(H)-hopane (βα-moretane/αβ-hopane) rise from 0.09 to 0.18 (Table 2). These relatively low ratios reflect an open sea with minimal contributions from terrestrial material. Pairs of C$_{27}$ hopanes [17α(H)-22,29,30-trisnorhopane (Tm) and 18α(H)-22,29,30-trisnorneohopane (Ts) or Ts/Tm ratios] may work as a facies parameter. This can
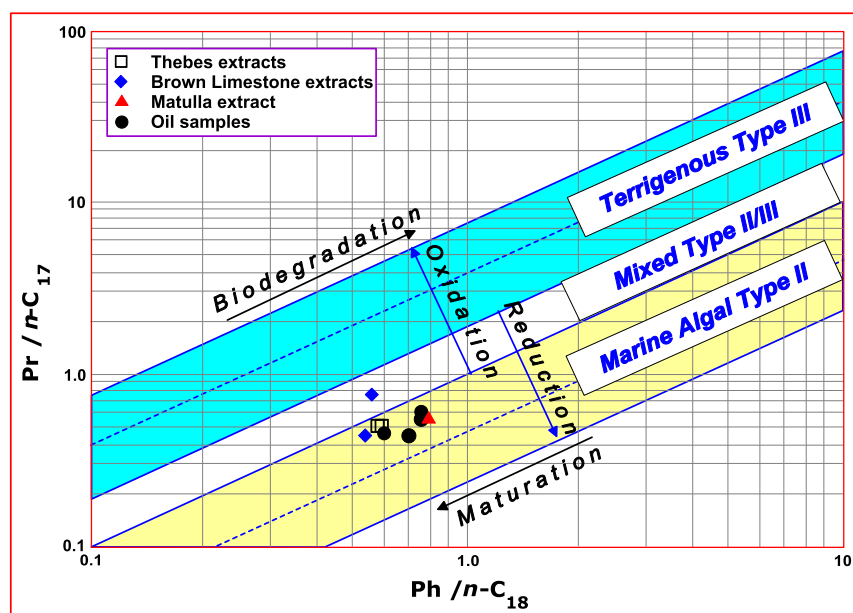
Figure 4 Pristane/n-C$_{17}$ versus phytane/n-C$_{18}$ for oil and extract samples from the Belayim Land oilfield (Peters et al., 1999).

Table 2 GC–MS results for the terpane (m/z 191) mass fragmentograms and their related ratios for source rock extracts and oil samples from the Belayim oilfields, central Gulf of Suez, Egypt.

No.	Well Name	Depth (m)	Formation	A	B	C	D	E	F	G	H	I	J
1	BL 113-A-15	3051	Thebes	0.15	0.90	0.12	0.46	0.58	0.97	0.57	2.08	0.05	0.77
2	BL 113-A-15	3083	Thebes	0.17	0.79	0.12	0.36	0.58	1.46	0.71	2.02	0.10	0.69
3	BL 113-A-15	3100	Thebes	0.23	0.77	0.18	0.33	0.54	1.27	0.78	2.20	0.05	0.66
4	BL 113-A-15	3136	Thebes	0.12	0.90	0.10	0.36	0.60	1.06	0.80	2.23	0.09	0.63
5	BL 113-A-15	3160	Thebes	0.13	0.90	0.10	0.36	0.59	0.96	0.72	2.03	0.10	0.61
6	BL 113-A-15	3172	Thebes	0.13	0.91	0.12	0.37	0.59	1.14	0.69	2.08	0.07	0.64
7	BL 113-A-15	3196	Thebes	0.15	0.93	0.13	0.37	0.59	1.25	0.66	2.11	0.06	0.69
8	BL 113-A-15	3220	Thebes	0.12	0.90	0.10	0.33	0.61	1.19	0.72	2.02	0.04	0.70
9	BL 113-A-15	3244	Thebes	0.13	0.82	0.10	0.33	0.60	1.17	0.73	1.98	0.04	0.68
10	BL 113-A-15	3256	Thebes	0.11	0.93	0.11	0.38	0.57	1.18	0.64	2.04	0.06	0.73
11	BL 113-A-15	3268	Thebes	0.11	0.93	0.09	0.42	0.58	1.06	0.68	2.11	0.08	0.73
12	BL 113-A-15	3274	Thebes	0.12	0.92	0.10	0.38	0.58	0.90	1.32	2.05	0.05	0.36
13	BL 113-A-15	3325	Brown Limestone	0.09	0.91	0.09	0.38	0.57	0.94	0.69	2.01	0.04	0.66
14	BL 113-A-15	3349	Brown Limestone	0.12	0.95	0.10	0.36	0.61	1.09	0.52	1.97	0.07	0.77
15	BL 113-A-15	3361	Brown Limestone	0.15	0.93	0.12	0.36	0.57	1.29	1.47	2.04	0.03	0.33
16	BL 113-A-15	3373	Brown Limestone	0.16	0.84	0.14	0.33	0.57	1.53	0.69	1.96	0.03	0.66
17	BL 113-A-15	3397	Matulla	0.12	0.84	0.12	0.38	0.57	1.17	0.67	2.07	0.07	0.66
18	BL 113-A-15	3406	Matulla	0.12	0.95	0.11	0.39	0.56	0.90	0.67	1.87	0.06	0.71
19	BL 113-A-15	3463	Matulla	0.10	0.93	0.09	0.39	0.56	0.98	0.64	1.99	0.06	0.69
20	BM-17	ND	ND	0.08	0.92	0.08	0.47	0.60	0.98	0.61	1.80	0.38	0.85
21	BM-29	2592	Rudeis	0.10	0.86	0.08	0.46	0.58	1.10	0.67	1.92	0.30	0.78
22	BM-49	ND	ND	0.09	0.88	0.08	0.49	0.61	1.02	0.71	1.79	0.34	0.76
23	BM-70	3450	Rudeis	0.11	0.84	0.09	0.42	0.59	1.04	0.53	1.90	0.28	0.77

A: Gammacerane/Hopane; B: C$_{29}$ Norhopane/C$_{30}$ Hopane; C: Moretane/Hopane; D: Ts/Tm Trisnorhopane; E: C$_{32}$ S/(S + R) Homohopane; F: C$_{35}$/C$_{34}$ Homohopane; G: C$_{24}$ Tetracyclic/C$_{26}$ Tricyclic terpanes; H: C$_{23}$/C$_{24}$ Tricyclic terpanes; I: C$_{19}$/C$_{23}$ Tricyclic terpanes; J: C$_{26}$/C$_{25}$ Tricyclic terpanes; ND: No data.

be interpreted from the ratio Ts/Tm. If this ratio is more than 0.5, this means that shale increases in the calcareous facies (Hunt, 1996). On the other hand, the Ts/Tm ratios recorded here (Table 2) range from 0.33 to 0.46 (< 0.5) indicating a marine carbonate depositional environment (Mello et al., 1988). A notable feature that distinguishes all the samples is the absence of oleanane which simply means that either no contribution of

oleanane precursor was present in the source rock, or that the source rocks are deposited far from angiosperm input.

High gammacerane and a high gammacerane index (Gammacerane/C$_{30}$ Hopane) are generally associated with highly reducing hypersaline conditions in both marine and lacustrine environments (Moldowan et al., 1985; Peters and Moldowan, 1993). Also, gammacerane is known to reflect water column

Table 3 GC–MS results for the sterane (*m/z* 217) mass fragmentograms and their related ratios for source rock extracts and oil samples from the Belayim oilfields, central Gulf of Suez, Egypt.

No.	Well name	Depth (m)	Formation	A	B	C	D	E	F	G	H	I	J	K	L
1	BL 113-A-15	3051	Thebes	49.2	15.3	35.6	0.30	0.40	1.38	0.61	3.57	1.63	0.77	1.59	42.6
2	BL 113-A-15	3083	Thebes	42.3	19.2	38.5	0.27	0.32	1.09	0.56	3.23	1.39	0.86	1.43	37.3
3	BL 113-A-15	3100	Thebes	43.5	17.0	39.5	0.22	0.26	1.10	0.53	3.20	1.12	0.81	1.32	28.8
4	BL 113-A-15	3136	Thebes	53.1	16.0	30.9	0.41	0.50	1.71	0.62	3.48	2.53	0.70	1.80	70.5
5	BL 113-A-15	3160	Thebes	46.9	22.2	30.9	0.39	0.55	1.51	0.62	2.62	2.17	0.67	1.63	65.0
6	BL 113-A-15	3172	Thebes	49.2	15.6	35.2	0.39	0.55	1.39	0.67	3.13	1.85	0.73	1.59	64.8
7	BL 113-A-15	3196	Thebes	50.8	14.7	34.6	0.37	0.54	1.46	0.70	3.02	2.10	0.68	1.71	57.7
8	BL 113-A-15	3220	Thebes	54.6	14.3	31.1	0.41	0.54	1.75	0.60	2.24	1.73	0.69	1.40	68.8
9	BL 113-A-15	3244	Thebes	47.6	18.5	33.8	0.42	0.51	1.40	0.52	2.96	1.14	0.71	1.08	71.8
10	BL 113-A-15	3256	Thebes	44.2	19.0	36.8	0.29	0.33	1.20	0.56	3.17	1.12	0.87	1.35	41.5
11	BL 113-A-15	3268	Thebes	50.2	12.7	37.0	0.39	0.50	1.35	0.70	2.65	1.87	0.75	1.71	65.2
12	BL 113-A-15	3274	Thebes	44.6	19.7	35.7	0.29	0.42	1.24	0.62	3.00	1.32	0.85	1.26	40.8
13	BL 113-A-15	3325	Brown Limestone	47.7	20.1	32.2	0.41	0.51	1.48	0.67	2.71	1.53	0.83	1.37	69.7
14	BL 113-A-15	3349	Brown Limestone	49.9	15.9	34.2	0.43	0.49	1.45	0.67	2.92	1.30	0.78	1.40	74.8
15	BL 113-A-15	3361	Brown Limestone	45.7	20.3	34.0	0.27	0.35	1.34	0.53	2.69	1.71	0.78	1.44	37.4
16	BL 113-A-15	3373	Brown Limestone	43.4	19.9	36.7	0.32	0.33	1.18	0.61	3.03	0.56	0.58	1.31	47.9
17	BL 113-A-15	3397	Matulla	41.2	18.7	40.1	0.27	0.36	1.02	0.56	3.51	1.10	0.76	1.34	37.6
18	BL 113-A-15	3406	Matulla	44.4	18.5	37.1	0.31	0.41	1.19	0.57	3.07	1.16	0.76	1.16	44.7
19	BL 113-A-15	3463	Matulla	49.1	14.7	36.2	0.39	0.46	1.35	0.66	2.63	1.34	0.79	1.41	63.4
20	BM-17	ND	ND	46.0	27.5	26.6	0.53	0.54	1.74	0.71	ND	1.12	0.94	0.79	53.0
21	BM-29	2592	Rudeis	47.1	24.3	28.6	0.53	0.56	1.65	0.25	ND	1.09	0.56	0.54	53.0
22	BM-49	ND	ND	47.0	28.3	24.7	0.56	0.55	1.92	0.70	ND	1.11	0.88	0.80	56.0
23	BM-70	3450	Rudeis	44.0	28.7	27.2	0.54	0.55	1.63	0.25	ND	1.10	0.62	0.62	49.0

A: %C_{27} $\alpha\alpha\alpha$R (*m/z* 217); B: %C_{28} $\alpha\alpha\alpha$R (*m/z* 217); C: %C_{29} $\alpha\alpha\alpha$R (*m/z* 217); D: S/(S + R) ($C_{29}\alpha\alpha\alpha$)(*m/z* 217); E: $\beta\beta$S/($\beta\beta$S + $\alpha\alpha$R) (C_{29}) (*m/z* 217); F: C_{27}/C_{29} ($\alpha\alpha\alpha$R) (*m/z* 217); G: Diasterane/$\alpha\alpha\alpha$ Sterane (C_{27}) (*m/z* 217); H: C_{30} S + R Sterane Index (*m/z* 218); I: C_{21}/C_{29} ($\alpha\alpha\alpha$ S + R) (*m/z* 217); J: Steranes/Hopanes = [(DIA27S + DIA27R + DIA28SA + DIA28SB + DIA28RA + DIA28RB + C_{27}S + $C_{27}\beta\beta$R + $C_{27}\beta\beta$S + C_{27}R + DIA29R + C_{28}S + $C_{28}\beta\beta$R + $C_{28}\beta\beta$S + C_{28}R + C_{29}S + $C_{29}\beta\beta$R + $C_{29}\beta\beta$S + C_{29}R)/(TS + TM + H28 + H29 + C_{29}TS + DH30 + H30 + H31R + H31S + H32R + H32S + H33R + H33S + H34R + H34S + H35R + H35S)]; K: Tricyclic Terpanes/Steranes = (TR19 + TR20 + TR21 + TR22 + TR23 + TR24 + TR25A + TR25B + TR26A + TR26B + TR28A + TR28B + TR29A + TR29B + TR30A + TR30B) / (DIA27S + DIA27R + DIA28SA + DIA28SB + DIA28RA + DIA28RB + C_{27}S + $C_{27}\beta\beta$R + $C_{27}\beta\beta$S + C_{27}R + DIA29R + C_{28}S + $C_{28}\beta\beta$R + $C_{28}\beta\beta$S + C_{28}R + C_{29}S + $C_{29}\beta\beta$R + $C_{29}\beta\beta$S + C_{29}R); L: %20S = $C_{29}(\alpha\alpha\alpha)$ 20S and 20R ratio (%); ND: No data.

stratification (e.g. Sinninghe Damsté et al., 1995). In this study, a strong gammacerane signal in most samples is not well defined. Moderate values for the gammacerane index ranging from 0.09 to 0.23 (Table 2) represent reducing conditions in different saline depositional environments (Moldowan et al., 1985). The majority of the analyzed samples show relatively high concentrations of C_{29} peaks with high C_{29}/C_{30} hopane ratios ranging from 0.77 to 0.95 (>0.6) (Table 2). This points to a marine environment (Peters et al., 2005) with organic rich carbonates and evaporites (Connan et al., 1986).

C_{27} and C_{28} steranes are derived from marine organisms, while the C_{29} steranes originate from higher plants. The investigated samples are characterized by low to slightly moderate abundances of C_{28}-ergostane and C_{29}-stigmastane comprising 12.7–22.2%, and 30.9–40.1% respectively, and relatively higher concentrations of C_{27}-cholestane comprising 41.2–54.6% of the total C_{27}–C_{29} regular steranes (Table 3). This signifies a greater marine input. The distribution of C_{27}, C_{28} and C_{29} $\alpha\alpha\alpha$(20R) steranes (Moldowan et al., 1985) is shifted toward C_{27} sterane, indicating that the majority of the extracts from the Thebes, Brown Limestone and Matulla formations may have been generated from predominantly marine organic matter. Confirmatory evidence for the marine proxies is provided by the C_{27}/C_{29} $\alpha\alpha\alpha$(20R) sterane ratio which rises from 1.02 to 1.75 (Table 3) and the sterane/17α-hopanes ratio was 0.58–0.87.

The extracts of the Eocene and Upper Cretaceous samples are characterized by the presence of a relatively low to moderate abundance (0.52–0.70) of the re-arranged steranes (Table 3). This is a characteristic feature of an anoxic, clay-poor, carbonate, marine depositional environment (Peters and Moldowan, 1993). This conclusion is consistent with the elevated C_{35}/C_{34} ratio of >1 (Table 2). The identification of C_{30} steranes in all samples supports their derivation from marine source rocks (Moldowan et al., 1985).

4.1.2. Maturity-related biomarkers

The composition of the extract samples shows that the non-hydrocarbons (NSO + asphaltene compounds) constitute 10.34–67.07% and hydrocarbons (saturates + aromatics) form 32.93–89.5% (Table 1). Such values indicate mature source rocks. The biologically-produced hopane precursors carry a 22R configuration at C-22, which is converted gradually to a mixture of 22R and 22S diastereomers. The C_{32} 22S/(22S + 22R) ratio rises from 0 to ∼0.6 (0.57–0.62 = equilibrium) (Seifert and Moldowan, 1980; Peters et al., 2005) during maturation. The Gulf extracts from the Eocene and Upper Cretaceous samples show values ranging from 0.54 to 0.61 (Table 2), indicating early to marginally mature source rocks. Isomerization at C-20 in the C_{29} 5α,14α,17α(H)-steranes causes 20S/(20S + 20R) to rise from 0 to ∼0.5 (0.52–0.55 = equilibrium)
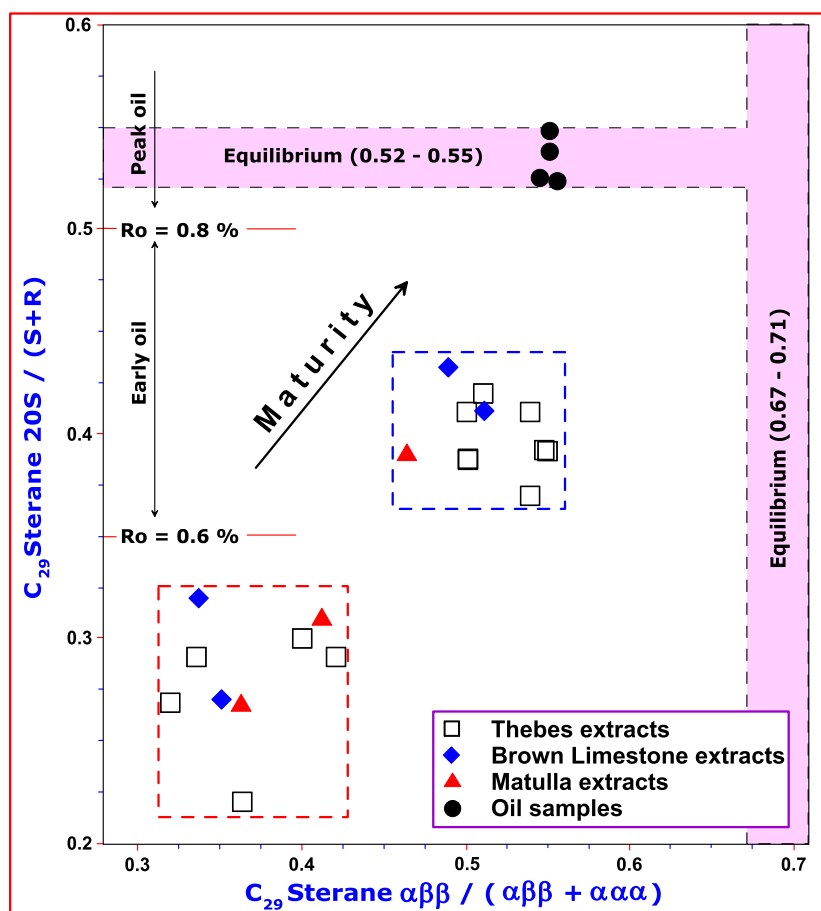
Figure 5   Relationship between $C_{29}\alpha\alpha\alpha20S/(S + R)$ and $C_{29}\alpha\beta\beta/(\alpha\beta\beta + \alpha\alpha\alpha)$ (Seifert and Moldowan, 1981).

with increasing thermal maturity (Seifert and Moldowan, 1986). The other isomerization at C-14 and C-17 in the C_{29} 20S and 20R regular sterane causes an increase in $\beta\beta/(\beta\beta + \alpha\alpha)$ from 0 to ~0.7 (0.67–0.71 = equilibrium) with increasing maturity (Seifert and Moldowan, 1986). The maturity parameter based on [20S/(20S + 20R) and $\beta\beta/(\beta\beta + \alpha\alpha)$]-$C_{29}$ steranes ranges from 0.22 to 0.43 and 0.26 to 0.55 (Table 3). Such values indicate low to early mature source rocks. The relationship between the sterane isomerization ratios C_{29} $\alpha\alpha\alpha$ 20S/(S + R) and C_{29} $\alpha\beta\beta/(\alpha\beta\beta + \alpha\alpha\alpha)$ is shown in Fig. 5. The plot shows two clusters, where the basal one is immature and located below the oil window. The other is marginally mature and can produce oil. This finding is supported from the C_{29} and C_{32} isomerization ratios.

4.2. Crude oil characterization

To assess the bulk composition of oil in any area, we have to consider some components such as API gravity, sulfur (wt%), nickel/vanadium and the stable carbon isotopes (Table 4). The oil samples recovered from the BM-17, BM-29, BM-49 and BM-70 wells have API gravities ranging from 25.0° to 31.11° (Table 4) indicating normal oils (Waples, 1985). The high sulfur content (> 0.5%) of the oil samples indicates that they have originated from clay-poor marine carbonates or evaporites deposited under anoxic conditions (Moldowan et al., 1985; Peters et al., 2005). The marine origin of these oils is deduced from the low nickel/vanadium (⩽1) ratios ranging from 0.19 to

0.29 (Table 4), confirming the findings of Elzarka et al. (1996) from the Gulf of Suez. The stable carbon isotope values for the saturated fraction range from −31.4 to −28.6‰; while the stable carbon isotope composition of the aromatic fraction ranges from −29.7 to −28.0‰ (Table 4). These values reveal that the crude oils of the Belayim Marine oilfield are generally derived from kerogen deposited in open marine environments (Tissot and Welte, 1984), confirming the findings of Rohrback (1983) who considered their derivation to be marine. The whole oil gas chromatogram (Fig. 3) is in full accordance with the one discussed earlier from the extracts. Similar results are reported above for the Pr/Ph, Pr/n-C_{17} and Ph/n-C_{18} ratios.

The C_7 analyses can be used in oil–oil and oil-source rock correlations and maturation studies. The crude oils appear to have low toluene/n-heptane and high n-heptane/methylcyclohexane which might indicate a water washing-suffering oil type (George et al., 2002) for the mature phase. The 6RP, 5RP and 3RP values represent terrestrial, marine and lacustrine organic matter content (Mango, 1994). These compounds could have been formed catalytically (Mango, 1994), and therefore a bacterial sulfate reduction (Wilkes et al., 2000) could have led to different values. In the present study, a number of parameters can corroborate a marine evaporitic environment; these include the high abundance of C_{23}, low C_{19}/C_{23}, C_{24} tetracyclic terpane, Ts/Tm ratio, high C_{29}/C_{30} hopane, high homohopane index, and high sterane (Table 2).

Table 4 Geochemical data and biomarker characteristics for crude oil samples from the Belayim Marine oilfield, central Gulf of Suez, Egypt.

Crude oil characteristics	BM-17	BM-29	BM-49	BM-70
Pay-zone	–	Rudeis	–	Rudeis
Depth (m)	–	2592	–	3450
API (American Petroleum Institute) gravity	31.1	29.0	28.3	25.0
$\delta^{13}C_{saturates}$	−30.3	−28.6	−31.4	−28.7
$\delta^{13}C_{aromatics}$	−29.7	−28.0	−29.6	−28.2
S (wt%)	1.23	1.90	1.32	2.00
Ni/V (ppm)	0.29	0.19	0.28	0.19
Pr/Ph	0.74	0.83	0.73	0.72
Pr/n-C_{17}	0.61	0.47	0.55	0.46
Ph/n-C_{18}	0.76	0.59	0.75	0.7
Parameters and ratios from C_7 compounds				
3RP%	32	36	35	37
5RP%	25	24	27	29
6RP%	43	40	38	34
Thompsons alteration vectors				
n-Heptane/methylcyclohexane	1.43	1.73	1.70	2.01
Toluene/n-heptane	0.49	0.48	0.46	0.35

To assess the maturity of oil, a number of parameters have to be considered. These include the bulk oil composition, saturate/aromatic ratio, the API gravity values, 22S/(22S + 22R) ratio of the C_{32}, and [20S/(20S + 20R)] and [ββ/(ββ + αα)]-C_{29} steranes (Tables 2–4). These parameters indicate that oil may have been expelled near the oil window (Fig. 5).

4.3. Oil-source rock correlation

Although few previous studies showed a good correlation of oils from the Thebes and Brown Limestone formations in the Belayim oilfields (Mostafa, 1993), the Matulla Formation received no attention as a source rock in these oilfields. The current geochemical data emphasize that a successful oil-source rock correlation was made between the source rocks and the oils, based on a multidisciplinary geochemical approach which included source rock depositional environment, kerogen type and levels of thermal maturity. The distributions of n-alkanes, terpanes and steranes, in addition to biomarker features (e.g. Pr/Ph, Ts/Tm, C_{29}/C_{30} hopane, C_{35}/C_{34} homohopane and the relative abundance of C_{27}–C_{28}–C_{29}), reveal a high similarity of kerogen type II to II/III. The oil samples and their equivalent source rocks also showed similar anoxic marine carbonate palaeoenvironmental conditions. In some instances it was difficult to correlate the maturity data of both the oils and their source rocks. This may be attributed to the influence of time on the maturation kinetics, and/or appreciable changes in temperature and pressure that prevailed during the deposition of the source rocks (Buryakovsky et al., 2005).

5. Conclusions

The Turonian–Eocene deposits retrieved from the Matulla, Brown Limestone and Thebes formations encountered in three wells located in the Belayim oilfields, central Gulf of Suez, Egypt have been studied. This included a detailed geochemical analysis of 19 cutting samples, as well as 4 oil samples. Conclusions may be summarized as follows:

1. The gas chromatograms, source and depositional environment-dependent biomarkers of both terpanes and steranes indicate their derivation from a marine algal source, with minor contributions from terrigenous inputs deposited under normal saline anoxic marine carbonate conditions.
2. The investigated rock units are immature to marginally mature as deduced from the combined evidence of biomarkers and maturation plots.
3. The recovered oil samples from the study area are normal oils. They were derived from clay-poor marine carbonates, deposited under normal saline anoxic conditions. The terrigenous contribution is minimal and signals of water washing have been recognized.
4. Maturity parameters based on molecular biomarkers indicate that the Belayim crude oils have experienced sufficient levels of thermal maturation relative to the extracts. Consequently, these oils could have been generated from the source rocks of the Brown Limestone and Thebes Formation in the deeper part of the kitchen area.

References

Alaug, A.S., Batten, D.J., Ahmed, A.F., 2013. Organic geochemistry, palynofacies and petroleum potential of the Mukalla formation (late Cretaceous), Block 16, eastern Yemen. Mar. Pet. Geol. 46, 67–91.

Al-Husseini, M.I., 2012. Late oligocene-early Miocene Nukhul sequence. Gulf of Suez and Red Sea. GeoArabia 17 (1), 17–44.

Alsharhan, A.S., 2003. Petroleum geology and potential hydrocarbon plays in the Gulf of Suez rift basin, Egypt. Am. Assoc. Pet. Geol. Bull. 87 (1), 143–180.

Aquino Neto, F.R., Trendel, J.M., Restle, A., Connan, J., Albrecht, P.A., 1983. Occurrence and formation of tricyclic and tetracyclic terpanes in sediments and petroleum. In: Bjorøy, M., Albrecht, P., Cornford, C. (Eds.), Advances in Organic Geochemistry 1981. John Wiley & Sons, New York, pp. 659–676.

Bakr, M.M.Y., Wilkes, H., 2002. The influence of facies and depositional environment on the occurrence and distribution of carbazoles and benzocarbazoles in crude oils: a case study from the Gulf of Suez, Egypt. Org. Geochem. 33, 561–580.

Barakat, A.O., El-Gayar, M.S., Mostafa, A.R., 1997. An organic geochemical investigation of crude oils from Egypt. Fuel Process. Technol. 51, 127–135.

Bosworth, W., McClay, K.R., 2001. Structural and stratigraphic evolution of the Gulf of Suez rift, Egypt: a synthesis. In: P.A. Ziegler, W. Cavazza, A.H.F.R. Robertson, S. Crasquin-Soleau, (Eds.), Peri-Tethyan Rift/Wrench Basins and Passive Margins. Mémoires du Muséum National d'Histoire Naturelle de Paris, Peri-Tethys Memoir 6, 186, pp. 567–606.

Buryakovsky, L., Eremenko, N.A., Gorfunkel, M.V., Chilingarian, G.V., 2005. Geology and geochemistry of oil and gas. In: Developments in Petroleum Science, vol. 52. Elsevier, Amsterdam, p. 91.

Connan, J., Bouroullec, J., Dessort, D., Albrecht, P., 1986. The microbial input in carbonate-anhydrite facies of sabkha palaeoenvironment from Guatemala: a molecular approach. Org. Geochem. 10, 29–50.

Didyk, B.M., Simoneit, B.R.T., Brassell, S.C., Eglinton, G., 1978. Organic geochemical indicators of palaeoenvironmental conditions of sedimentation. Nature 272, 216–222.

Egypt Country Analysis Briefs, 2009. Country analysis briefs (Oil and natural gas energy annual report, Egypt). February, 2009 (internet report).

El Diasty, W.Sh., Peters, K.E., 2014. Genetic classification of oil families in the central and southern sectors of the Gulf of Suez, Eypt. J. Pet. Geol 37 (2), 105–126.

Elzarka, M.H., Waly, M., Abdel-Aziz, M., Shahin, A.N., 1996. Genesis of the Eocene crude in the Gulf of Suez: an oil-rock correlation based on porphyrin contents. Proceedings of the 13th Petroleum Exploration and Production Conference, Egyptian General Petroleum Corporation, Cairo, Egypt, 447–474.

Ganz, H., Kalkreuth, W., Ganz, S.H., Öner, F., Pearson, M.J., Wehner, H., 1990. Infrared analysis-state of the art. Berl. Geowissenschaftliche Abhandlungen Reihe A 120 (2), 1011–1026.

George, S.C., Boreham, C.J., Minifie, S.A., Teerman, S.C., 2002. The effect of minor to moderate biodegradation on C_5 to C_9 hydrocarbons in crude oils. Org. Geochem. 33, 1293–1317.

Hunt, J.M., 1996. Petroleum Geochemistry and Geology, Second ed. Freeman, New York.

Mango, F.D., 1994. The origin of light hydrocarbons in petroleum: ring preference in the closure of carbocyclic rings. Geochim. Cosmochim. Acta 58, 895–901.

Mann, A.L., Goodwin, N.S., Lowe, S., 1987. Geochemical characteristics of lacustrine source rocks: a combined palynological/molecular study of a tertiary sequence from offshore China. Proceedings of the Indonesian Petroleum Association, 16th Annual Convention, 1, Indonesian Petroleum Association, Jakarta, 1, 241–258.

Mello, M.R., Gaglianone, P.C., Brassell, S.C., Maxwell, J.R., 1988. Geochemical and biological marker assessment of depositional environments using Brazilian offshore oils. Mar. Pet. Geol. 5, 205–223.

Meshref, W.M., 1990. Tectonic framework. In: Said, R. (Ed.), The Geology of Egypt. Balkema, Rotterdam, pp. 113–155.

Moldowan, J.M., Seifert, W.K., Gallegos, E.J., 1985. Relationship between petroleum composition and depositional environment of petroleum source rocks. Am. Assoc. Pet. Geol. Bull. 69, 1255–1268.

Mostafa, A.R., 1993. Organic geochemistry of source rocks and related crude oils in the Gulf of Suez, Egypt. Berl. Geowissenschaftliche Abhandlungen Reihe A 147, 163.

Ourisson, G., Albrecht, P., Rohmer, M., 1982. Predictive microbial biochemistry- from molecular fossils to prokaryotic membranes. Trends Biochem. Sci. 7, 236–239.

Palacas, J.G., Donald, E.A., King, J.D., 1984. South Florida Basin – a prime example of carbonate source rocks of petroleum. In: J.G. Palacas, (Ed.), Petroleum Geochemistry and Source Rock potential of Carbonate Rocks. American Association of Petroleum Geologists Studies in Geology 18, pp. 71–96.

Peters, K.E., Fraser, T.H., Amris, W., Rustanto, B., Hermanto, E., 1999. Geochemistry of crude oils from eastern Indonesia. Am. Assoc. Pet. Geol. Bull. 83, 1927–1942.

Peters, K.E., Moldowan, J.M., 1993. The Biomarker Guide. Prentice-Hall, Englewood Cliffs, New Jersey, p. 363.

Peters, K.E., Walters, C.C., Moldowan, J.M., 2005. The Biomarker Guide, 2nd Edition, Part I, "Biomarkers and Isotopes in the Environmental and Human History", and Part II "Biomarkers and Isotopes in Petroleum Exploration and Earth History". Cambridge University Press, Cambridge, p. 1155.

Petrobel, 2005. Belayim Marine and Belayim Land type logs, Exploration Department (internal report), Petrobel Company.

Plaziat, J.-C., Montenat, C., Barrier, P., Janin, M.-C., Orszag-Sperber, F., Philobbos, E., 1998. Stratigraphy of the Egyptian syn-rift deposits: correlation between axial and peripheral sequences of the north-western Red Sea and Gulf of Suez and their relations with tectonics and eustasy. In: Purser, B.H., Bosence, D.W.J. (Eds.), Sedimentation and Tectonics in Rift Basins. Red Sea-Gulf of Aden, pp. 211–222.

Rohrback, B.G., 1983. Crude oil geochemistry of the Gulf of Suez. In: Bjorøy, M., Albrecht, P., Cornford, C., et al. (Eds.), Advances in Organic Geochemistry, 1981. Wiley, Chichester, pp. 39–48.

Roushdy, M.I., El Nady, M.M., Mostafa, Y.M., El Gendy, N.Sh., Ali, H.R., 2010. Biomarkers characteristics of crude oils from some oilfields in the Gulf of Suez, Egypt. J. Am. Sci. 6 (11), 911–925.

Schütz, K.I., 1994. Structure and stratigraphy of the Gulf of Suez, Egypt. In: Landon, S.M. (Ed.), . In: Interior Rift Basins, vol. 59. American Association of Petroleum Geologists, pp. 57–96.

Seifert, W.K., Moldowan, J.M., 1980. The effect of thermal stress on source-rock quality as measured by hopane stereochemistry. Phys. Chem. Earth 12, 229–237.

Seifert, W.K., Moldowan, J.M., 1981. Paleoreconstruction by biological markers. Geochim. Cosmochim. Acta 45, 783–794.

Seifert, W.K., Moldowan, J.M., 1986. Use of biological markers in petroleum exploration. In: Johns, R.B. (Ed.), Methods in Geochemistry and Geophysics 24. Elsevier, Amsterdam, pp. 261–290.

Sinninghe Damsté, J.S., Kenig, F., Koopmans, M.P., Köster, J., Schouten, S., Hayes, J.M., de Leeuw, J.W., 1995. Evidence for gammacerane as an indicator of water column stratification. Geochim. Cosmochim. Acta 59, 1895–1900.

ten Haven, H.L., Peakman, T.M., Rullkötter, J., 1992. Early diagenetic transformation of higher-plant triterpenoids in deep-sea sediments from Baffin Bay. Geochim. Cosmochim. Acta 56, 2001–2024.

Tissot, B.P., Welte, D.H., 1984. Petroleum formation and occurrence, Second ed. Springer, New York, p. 699.

Waples, D.W., 1985. Geochemistry in Petroleum Exploration. International Human Resources Development Corporation, Boston, p. 232.

Wilkes, H., Boreham, C., Harms, G., Zengler, K., Rabus, R., 2000. Anaerobic degradation and carbon isotopic fractionation of alkylbenzenes in crude oil by sulphate-reducing bacteria. Org. Geochem. 31 (1), 101–115.

Young, M.J., Gawthorpe, R.L., Sharp, I.R., 2000. Sedimentology and sequence stratigraphy of a transfer zone coarse-grained fan delta, Miocene Suez Rift, Egypt. Sedimentology 47, 1081–1104